Terahertz time-domain spectroscopy and imaging of artificial RNA

Bernd M. Fischer, Matthias Hoffmann, and Hanspeter Helm

Department of Molecular and Optical Physics, Freiburg Materials Research Center, Universität Freiburg, Hermann-Herder-Strasse 3, D-79104 Freiburg, Germany

Rafal Wilk, Frank Rutz, Thomas Kleine-Ostmann and Martin Koch

Institut für Hochfrequenztechnik, Technische Universität Braunschweig, Schleinitzstrasse 22, D-38106 Braunschweig, Germany

Peter Uhd Jepsen

Research Center COM, Technical University of Denmark, DK-2800 Kgs. Lyngby, Denmark

jepsen@com.dtu.dk

Abstract: We use terahertz time-domain spectroscopy (THz-TDS) to measure the far-infrared dielectric function of two artificial RNA single strands, composed of polyadenylic acid (poly-A) and polycytidylic acid (poly-C). We find a significant difference in the absorption between the two types of RNA strands, and we show that we can use this difference to record images of spot arrays of the RNA strands. Under controlled conditions it is possible to use the THz image to distinguish between the two RNA strands. We discuss the requirements to sample preparation imposed by the lack of sharp spectral features in the absorption spectra.

OCIS codes: (300.6270) Spectroscopy, far infrared; (170.3880) Medical and biological imaging.

References and links

1. A. Doria, G. P. Gallerano, E. Giovenale, G. Messina, A. Lai, A. Ramundo-Orlando, V. Spotsato, M. D'Arienzo, A. Perrotta, M. Romano, M. Sarti, M. R. Scarfi, I. Spassovsky, and O. Zeni, "THz radiation studies on biological systems at the ENEA FEL facility," Infrared Phys. Technol. **45,** 339 (2004)
2. E. Pickwell, B. E. Cole, A. J. Fitzgerald, V. P. Wallace, and M. Pepper, "Simulation of terahertz pulse propagation in biological systems," Appl. Phys. Lett. **84,** 2190 (2004)
3. S. W. Smye, J. M. Chamberlain, A. J. Fitzgerald, and E. Berry, "The interaction between terahertz radiation and biological tissue," Phys. Med. Biol. **46,** R101 (2001)
4. E. R. Brown, J. E. Bjarnason, T. L. J. Chan, A. W. M. Lee, and M. A. Celis, "Optical attenuation signatures of *Bacillus subtillis* in the THz region," Appl. Phys. Lett. **84,** 3438 (2004)
5. T. Globus, M. Bykhovskaia, D. Woolard, and B. Gelmont, "Sub-millimetre wave absorption spectra of artificial RNA molecules," J. Phys. D **36,** 1314 (2003)
6. D. L. Woolard, T. R. Globus, B. L. Gelmont, M. Bykhovskaia, A. C. Samuels, D. Cookmeyer, J. L. Hesler, T. W. Crowe, J. O. Jensen, J. L. Jensen, and W. R. Loerop, "Submillimeter-wave phonon modes in DNA macromolecules," Phys. Rev. E **65,** 051903 (2002)
7. R. M. Woodward, V. P. Wallace, D. D. Arnone, E. H. Linfield, and M. Pepper, "Terahertz pulsed imaging of skin cancer in the time and frequency domain," J. Biol. Phys. **29,** 257 (2003)
8. J. Xu, G. J. Ramian, Jhenny F. Galan, Pavlos G. Savvidis, A. M. Scopatz, R. R. Birge, S. James Allen, and K. W. Plaxco, "Terahertz circular dichroism spectroscopy: A potential approach to the *in situ* detection of life's metabolic and genetic machinery," Astrobiol. **3,** 489 (2003)
9. A. Markelz, S. Whitmire, J. Hillebrecht, and R. Birge, "THz time domain spectroscopy of biomolecular conformational modes," Phys. Med. Biol. **47,** 3797 (2002)

#7174 - $15.00 USD Received 15 April, 2005; revised 14 June, 2005; accepted 23 June, 2005

10. S. E. Whitmire, D. Wolpert, A. G. Markelz, J. R. Hillebrecht, J. Galan, and R. R. Birge, "Protein flexibility and conformational state: A comparison of collective vibrational modes of wild-type and D96N bacteriorhodopsin," Biophys. J. **85,** 1269 (2003)
11. M. Walther, B. M. Fischer, and P. Uhd Jepsen, "Noncovalent intermolecular forces in polycrystalline and amorphous saccharides in the far infrared," Chem. Phys. **288,** 261 (2003)
12. F. Rutz, R. Wilk, T. Kleine-Ostmann, and M. Koch, "Experimental and theoretical study of the THz absorption spectra of selected tripeptides," Proc. SPIE **5727,** (2005)
13. M. Brucherseifer, M. Nagel, P. Haring Bolivar, H. Kurz, A. Bosserhoff, and R. Büttner, "Label-free probing of the binding state of DNA by time-domain terahertz sensing," Appl. Phys. Lett. **77,** 4049 (2000)
14. M. Nagel, P. Haring Bolivar, M. Brucherseifer, H. Kurz, A. Bosserhoff, and R. Büttner, "Integrated THz technology for label-free genetics diagnostics," Appl. Phys. Lett. **80,** 154 (2002)
15. M. Walther, B. Fischer, M. Schall, H. Helm, and P. Uhd Jepsen, "Far-infrared vibrational spectra of all-trans, 9-cis, and 13-cis retinal measured by THz time-domain spectroscopy," Chem. Phys. Lett. **332,** 389 (2000)
16. M. Schall, M. Walther, and P. Uhd Jepsen, "Fundamental and second-order phonon processes in CdTe and ZnTe," Phys. Rev. B **64,** 094301 (2001)
17. P. Knobloch, C. Schildknecht, T. Kleine-Ostmann, M. Koch, S. Hoffmann, M. Hofmann, E. Rehberg, M. Sperling, K. Donhuijsen, G. Hein, and K. Pierz, "Medical THz imaging: an investigation of histopathological samples," Phys. Med. Biol. **47,** 3875 (2002)
18. P. Uhd Jepsen and B. M. Fischer, "Dynamic range in terahertz time-domain transmission and reflection spectroscopy," Opt. Lett. **30,** 29 (2005)
19. M. L. T. Asaki, A. Redondo, T. A. Zawodzinski, and A. J. Taylor, "Dielectric relaxation of electrolyte solutions using terahertz transmission spectroscopy," J. Chem. Phys. **116,** 8469 (2002)

1. Introduction

In the recent years there has been considerable interest in application of the terahertz frequency range (0.1 - 5 THz) for detection and characterization of biological material, with emphasis on interaction between electromagnetic radiation and biological material [1, 2, 3], stand-off detection of biological warfare agents [4], analysis of low-frequency vibrations in RNA- and DNA strands [5, 6] and proteins [9, 10], as well as detection of skin cancer by THz imaging [7]. The interaction mechanism leading to absorption in the THz frequency range in biological material is still under debate, but it seems clear that intramolecular as well as intermolecular interactions mediated via hydrogen bonds and weak interactions such as van der Waals forces play an important role.

Recently it was suggested that THz circular dichroism (TCD) spectroscopy could be a universal tool for the detection of biological material [8]. Based on the strong tendency of biological processes to produce molecules with a handedness the authors argue that TCD spectroscopy may be a universal method for the detection of life processes, for instance in extraterrestrial environments.

Many biomolecular crystals exhibit strong and specific absorption features in their dielectric spectra, arising from intramolecular vibrations and from phonon modes of the molecular crystal lattice [11, 12]. Biological systems with little or no long-range ordering of the constituent molecules, in contrast, exhibit little or no structure in their THz dielectric properties. This may firstly arise from the missing of defined phonon modes and secondly from an inhomogeneous broadening of the intramolecular vibrations.

Yet, in spite of the lack of characteristic absorption features in the THz region it is possible to apply THz technology to the identification of the binding state of DNA [13]. In this case the highest sensitivity has been obtained by loading a planar THz resonator with the sample material. Experiments have indicated that the modification of the effective dielectric load leads to a measurable shift of the resonance frequency [14].

In this study we investigate the possibility to use the THz absorption spectrum of two different RNA polymer strands, polyadenylic acid (poly-A) and polycytidylic acid (poly-C), for identification purposes. We are especially interested in applications where the material is spotted in arrays on a disposable substrate. It turns out that the preparation of the sample material

#7174 - $15.00 USD Received 15 April, 2005; revised 14 June, 2005; accepted 23 June, 2005

is important when interpreting the results. We therefore performed independent spectroscopic measurements in two laboratories, using a variety of sample preparation methods.

2. Materials and sample preparation

We have used commercially available poly-A and poly-C potassium salts (Sigma-Aldrich, product numbers P9403 and P4903). The chemical structures of the polymers are shown in Fig. 1.

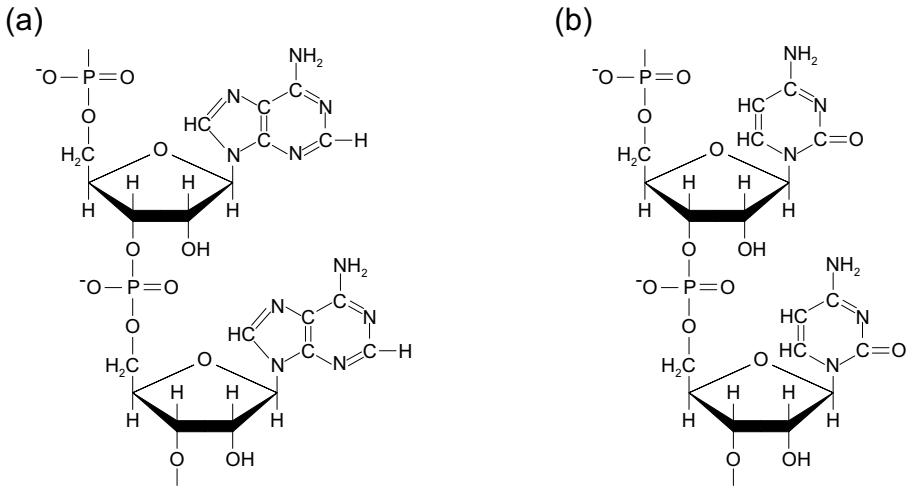

Fig. 1. Chemical structure of (a) polyadenylic acid (poly-A) and (b) polycytidylic acid (poly-C). The negative charge of the backbone is neutralized by potassium ions.

According to the manufacturer the molecular weight of the polymer chains is distributed between 10^5 g/mol and $2 \cdot 10^6$ g/mol, with the greatest density in the region $2 \cdot 10^5$ g/mol to $7 \cdot 10^5$ g/mol. This corresponds to polymer chains with lengths of approximately 600-2000 A or C units. The sample material is delivered in a low-density powder form.

One of the aims of the present work is to investigate the influence of the sample preparation method. Therefore we prepared the sample material in various manners as described below. An overview of the samples is presented in Table 1.

The samples FR-1 and FR-2 were prepared for spectroscopy by pressing of the sample material in a die at approximately 0.74 kbar pressure. The resulting samples were mechanically stable with thicknesses of 300 and 180 μm, respectively. The samples BR-1 and BR-2 were prepared with a pressure of 0.38 kbar, and had thicknesses of 150 μm.

The samples FR-3 and FR-4 were prepared for spectroscopy as free-standing films of poly-A and poly-C by dissolving the powder material in deionized water. The solution was distributed over a 1-cm^2 area on a nonpolar polymer substrate. The substrate was the commercially available cyclic olefin TOPAS (Greiner Bio-One), which is transparent and dispersion-free in the THz frequency range. After drying by evaporation in a dry atmosphere the film could be lifted off the substrate. The resulting film thicknesses were 100 and 45 μm, respectively.

The sample BR-3 was prepared for spectroscopy by repeated application of dissolved sample material at the same spot on a TOPAS substrate. Two spots containing poly-A and two spots containing poly-C were prepared. The diameter of each spot was 1.5 mm, and the spot thickness was estimated to be 100 μm. The sample BR-4 was a pellet pressed at 0.38 kbar, prepared with 6 mg of poly-A and 6 mg of poly-A located at different positions in a matrix consisting of 150

#7174 - $15.00 USD Received 15 April, 2005; revised 14 June, 2005; accepted 23 June, 2005

Table 1. Overview of the samples used in the study. The preparation methods are described in the text. Samples denoted FR-1 - FR-6 were prepared and characterized in Freiburg, and samples denoted BR-1 - BR-4 were prepared and characterized in Braunschweig.

Sample ID	Ingredients	Thickness	Preparation method	Usage
FR-1	poly-A	300 μm	pellet	spectroscopy
FR-2	poly-C	180 μm	pellet	spectroscopy
FR-3	poly-A	100 μm	freestanding film	spectroscopy
FR-4	poly-C	45 μm	freestanding film	spectroscopy
FR-5	poly-A/poly-C	40-50 μm	4 x 4 array	imaging
FR-6	poly-A/poly-C	40-50 μm	4 x 2 array	imaging
BR-1	poly-A	150 μm	pellet	spectroscopy
BR-2	poly-C	150 μm	pellet	spectroscopy
BR-3	poly-A/poly-C	100 μm	2 x 2 array	spectroscopy
BR-4	poly-A/poly-C		inclusions in pellet	imaging

mg polyethylene powder. The polyethylene was high-density, spectroscopic grade material, purchased from Sigma-Aldrich (Fluka 81149).

We prepared the sample FR-5 for THz imaging by spotting small liquid volumes in a 4 x 4 array of alternating poly-A and poly-C on a TOPAS substrate. Each spot was deposited with 2 μL of deionized water containing 0.2 mg material. The diameter of each spot was 1 mm. The sample FR-6 was prepared in a similar manner with a dilution series of spots containing between 0.2 mg and 0.02 mg poly-A or poly-C. The dimensions and topology of the dried spots on the surfaces of the samples FR-5 and FR-6 were characterized with a mechanical surface profiler (Tencor P-16).

3. Experimental methods

We used standard free-space terahertz time-domain spectroscopy (THz-TDS) to characterize our samples. We used two independent spectroscopy systems located in laboratories in Freiburg and in Braunschweig in order to study the effect of differences in sample preparation and implementation details of the THz-TDS system. Both THz-TDS systems are based on photoconductive antennas for generation and detection of the far-infrared light [15, 16, 17]. A schematic overview of the setup is shown in Fig. 2.

In brief, the dielectric properties, here represented as the absorption coefficient $\alpha(\nu)$ and index of refraction $n(\nu)$, are determined in transmission THz-TDS by measuring a sample pulse trace $E_{sam}(t)$ and a reference pulse trace $E_{ref}(t)$. Synchronized ultrafast photoconductive generation and sampling is used to directly measure the temporal profile of the electric field of each pulse trace. The pulses are recorded with and without the sample material placed at an intermediate focal plane in the beam path of the spectrometer. The two pulse traces are then Fourier transformed to the frequency domain to obtain their complex-valued spectra. From the ratio A and phase difference $\Delta\phi$ of these spectra the dielectric properties of the sample material can be extracted, taking into account Fresnel losses at the interfaces of the sample material.

With this method the index of refraction and the absorption coefficient for a free-standing sample is calculated as

$$n(\nu) \quad = \quad 1+\frac{c}{2\pi\nu d}\Delta\phi(\nu)\,, \tag{1}$$

#7174 - $15.00 USD Received 15 April, 2005; revised 14 June, 2005; accepted 23 June, 2005

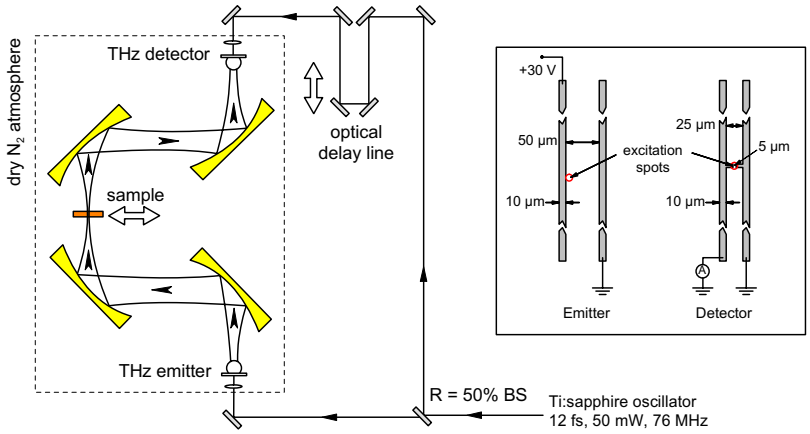

Fig. 2. Schematic illustration of the experimental setup for THz time-domain spectroscopy (THz-TDS). The inset shows details about the photoconductive antennas.

$$\alpha(\nu) \quad = \quad -\frac{2}{d}\ln\left[A(\nu)\frac{(n(\nu)+1)^2}{4n(\nu)}\right] , \tag{2}$$

where d is the thickness of the sample. In this analysis we have assumed that scattering effects can be neglected. This approximation is only valid for plane, homogeneous samples. Scattering of radiation away from the propagation axis will manifest itself as increased apparent absorption in the analysis outlined above. Therefore a comparison of results obtained in different experimental setups and on different samples can be used to estimate the influence of scattering on our spectroscopic results.

In general, we can measure the absorption coefficient and index of refraction of the samples in the frequency range 0.1 - 4.0 THz, with a frequency resolution of 15 GHz (< 0.5 cm^{-1}). Care was taken to operate the spectrometers below saturation of their dynamic range [18].

4. Spectroscopic results

In order to establish the spectral characteristics of the samples we measured the absorption coefficient and the index of refraction of poly-A and poly-C pressed into plane pellets. In Fig. 3 the spectra recorded in Braunschweig are shown, and in Fig. 4 the spectra recorded in Freiburg are shown. In Fig. 3 the spectra indicated by symbols correspond to individual measurements, whereas the traces represented by solid lines show the average value. In Fig. 4 the solid lines represent the average value of 10 individual measurements. The error bars indicate the statistical standard deviation of the average value, based on the standard deviation of the measurements in the time domain.

The results obtained in the two laboratories on poly-A and poly-C pellets are similar. The absorption coefficient of both materials increases in an almost linear fashion in the region between 0.1 and 2.5 THz. The data show that poly-C absorbs stronger than poly-A at all frequencies. No distinct spectral features are observed. A constant scaling factor can overlap the spectra of poly-A and poly-C completely. This shows that although we observe a difference in the absorption of poly-A and poly-C it is important to know the density of the sample material before any identification of the material based on its THz absorption spectrum can be made.

The index of refraction of poly-C is approximately 10 percent larger than that of poly-A. The

#7174 - $15.00 USD Received 15 April, 2005; revised 14 June, 2005; accepted 23 June, 2005

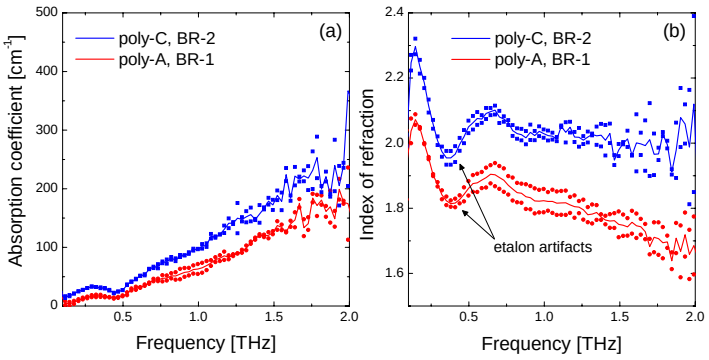

Fig. 3. (a) Absorption coefficient and (b) index of refraction of pressed pellets (samples BR-1 and BR-2) of poly-A and poly-C at room temperature in the frequency range 0.15-2.0 THz. Traces represented by symbols correspond to individual measurements whereas traces represented by full lines show the average value.

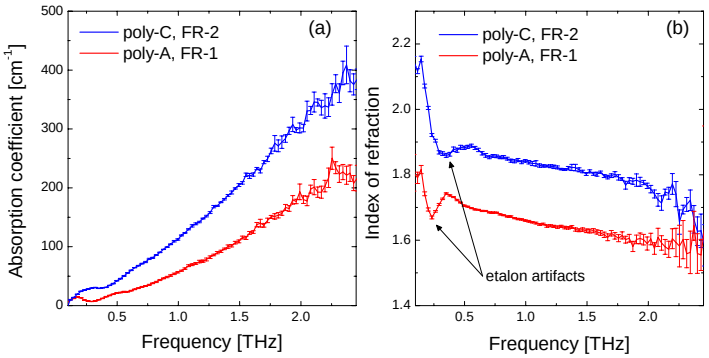

Fig. 4. (a) Absorption coefficient and (b) index of refraction of pressed pellets (samples FR-1 and FR-2) poly-A and poly-C at room temperature in the frequency range 0.1-2.45 THz. The vertical error bars indicate the standard deviation of the mean values in each experiment.

#7174 - $15.00 USD Received 15 April, 2005; revised 14 June, 2005; accepted 23 June, 2005

strong oscillatory feature at low frequencies observed in all measurements is due to multiple reflections of the sample beam inside the relatively thin samples. We see this etalon effect only at low frequencies where the absorption is low. At higher frequencies where the absorption is substantial the THz field is absorbed before multiple reflections can occur.

In Fig. 5 the measured absorption coefficient and index of refraction of poly-A and poly-C prepared from solution as freestanding films (samples FR-3 and FR-4, respectively) is shown.

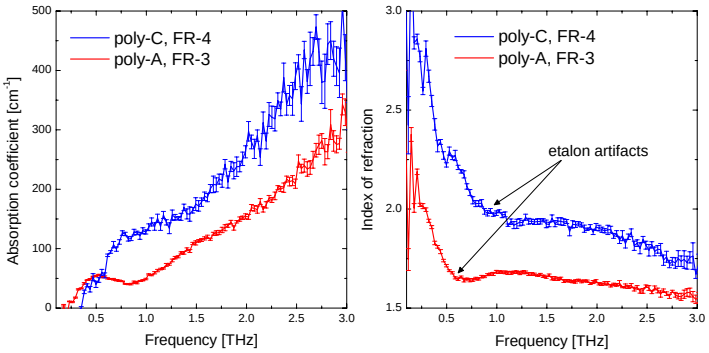

Fig. 5. (a) Absorption coefficient and (b) index of refraction of free-standing, dry films of poly-A and poly-C (samples FR-3 and FR-4) at room temperature in the frequency range 0.1-3.0 THz. The vertical error bars indicate the standard deviation of the mean values in each experiment.

Again the solid lines represent the average value of 10 individual measurements. The error bars indicate the statistical standard deviation of the average value within this measurement. We obtain slightly lower absorption coefficients compared to the values of the samples FR-1 and FR-2 as well as BR-1 and BR-2. The indices of refraction of the freestanding films is slightly higher than those of FR-1 and FR-2, respectively, and slightly lower than the respective refractive indices BR-1 and BR-2. This discrepancy can be caused either by mechanical or chemical differences arising from the different sample preparation methods. Again we interpret the oscillations at low frequencies simply as etalon effects.

Finally we measured the absorption coefficient of thick spots of dried poly-A and poly-C (sample BR-3). Owing to the small spot size we expect diffraction effects to play an important role in this measurement. The results are shown in Fig. 6. The curves displayed as symbols represent individual measurements on a single spot of either poly-A and poly-C whereas the solid lines represent the average absorption coefficient. We observe significant oscillations in the measured absorption. Based on the spectra recorded on larger samples of the same material we are, however, able to conclude that these oscillations originate from the geometry of the sample rather than from the dielectric response of the sample material itself. At 1 THz the wavelength of the probe light is 300 μm. Since the spot diameter is only 1.5 mm (5 wavelengths) it is not surprising that diffraction effects may influence the measurement.

5. Imaging of RNA spot arrays

Having established that we can use THz time-domain spectroscopy to distinguish between different biopolymers it is interesting to determine if this differentiation can be used in THz imaging as well. For this purpose we prepared targets for imaging that challenges the spatial resolution obtainable with a THz-TDS imaging system based on free-space propagation and aperture-less focusing of the THz beam. In Fig. 7(a) a THz transmission image of the sample

#7174 - $15.00 USD Received 15 April, 2005; revised 14 June, 2005; accepted 23 June, 2005

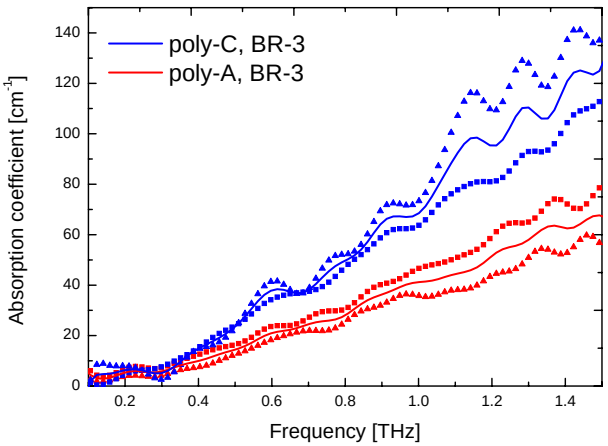

Fig. 6. Absorption coefficient of spots of poly-A and poly-C on the substrate surface of sample BR-3 at room temperature in the frequency range 0.1-1.5 THz. Traces represented by symbols correspond to individual measurements whereas traces represented by full lines show the average value.

BR-4 is shown, and in Fig. 7(b) a photograph of the same sample is shown for comparison. The

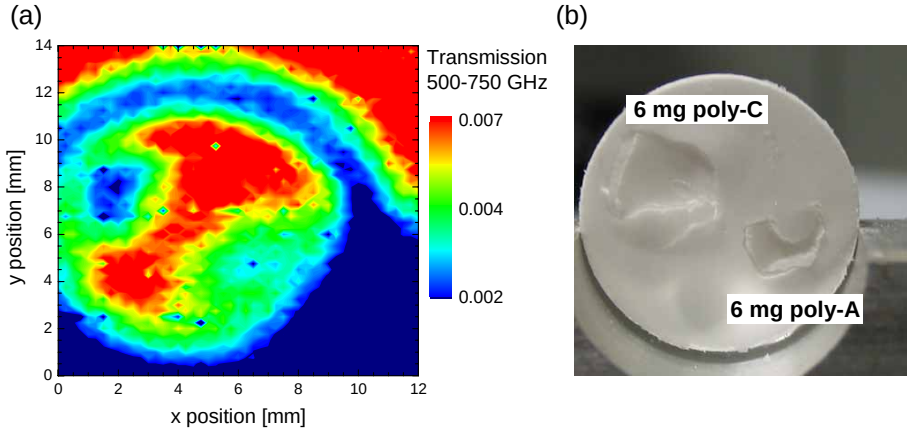

Fig. 7. (a) THz transmission image of the polyethylene pellet containing 6 mg of poly-A and 6 mg of poly-C at different regions (sample BR-4). (b) Photograph of the sample for comparison, indicating the location of the sample material.

image was recorded by scanning of the sample across the focus of the THz beam while recording the temporal shape of the THz pulse at each pixel. The image was then color-coded according to the integrated transmission in the 0.5–0.75 THz frequency range. The image shows lower transmission in the regions of the sample material, and the smallest transmission is observed in the region where the poly-C powder is located. This is in agreement with the spectroscopic results shown above. The region of no transmission in the lower part of the image is the shadow region of the sample mount, also visible in the photograph of the sample.

In Fig. 8 we show the THz image of the sample FR-5. Nominally the sample consisted of

#7174 - $15.00 USD Received 15 April, 2005; revised 14 June, 2005; accepted 23 June, 2005

a 4x4 array of spots. Two of the spots, however, were removed from the substrate in order

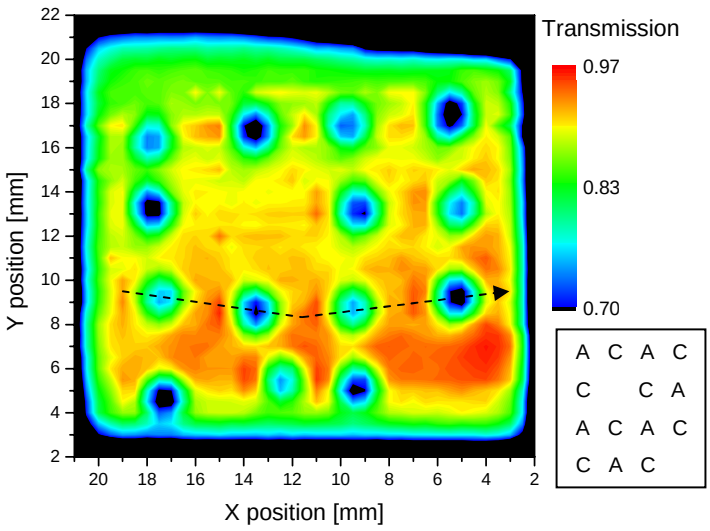

Fig. 8. THz transmission image of the sample FR-5, again showing stronger absorption in poly-C compared to poly-A. Each spot contained 200 μg of either poly-A or poly-C in alternating order, as indicated in the diagram to the right. The dashed line indicates the scan path of the surface profiler.

to identify the orientation of the substrate in the image. The spot in the top left corner of the image contains poly-A. The THz image was formed by the frequency-integrated transmission over the full bandwidth of the probe pulse. The poly-C spots lead to a substantial transmission drop of 30%, whereas the poly-A spots reduce the transmission by 20%. In order to verify that the differences observed in the image between the different spot types is related to differences in the sample material and not caused by differences in spot size or thickness we performed surface height scans with a mechanical surface profiler of the sample after the measurement. In Fig. 9 we show the surface profile of the sample FR-5 along the path indicated in Fig. 8. Notice that the horizontal scale of the plot is much smaller than the vertical scale. The spots all have approximately the same height, diameter, and topology. The average height is 40-50 μm, and the diameter is slightly larger than 1 mm. There is a pronounced height enhancement at the edges of the spots, which is normal for this type of spotting. We expect that if the topology of the spots are not similar then diffraction effects may influence the appearance of the image strongly.

Finally, we recorded a series of diluted spots on the sample FR-6, as shown in Fig. 10. The amount of sample material in each spot is indicated in the figure, and ranges from 20 μg to 200 μg. As indicated by the strong signal attenuation observed in the image of the 4x4 spot array in Fig. 8 we can reduce the amount of sample material by approximately an order of magnitude before the signal disappears in the present form of the experiment. The contrast between poly-A and poly-C degrades rapidly with decreasing amount of sample material.

6. Discussion and conclusions

We have investigated the possibility of using THz time-domain spectroscopy and imaging to detect differences between biomolecules, in particular the single-stranded RNA polymers poly-

#7174 - $15.00 USD Received 15 April, 2005; revised 14 June, 2005; accepted 23 June, 2005

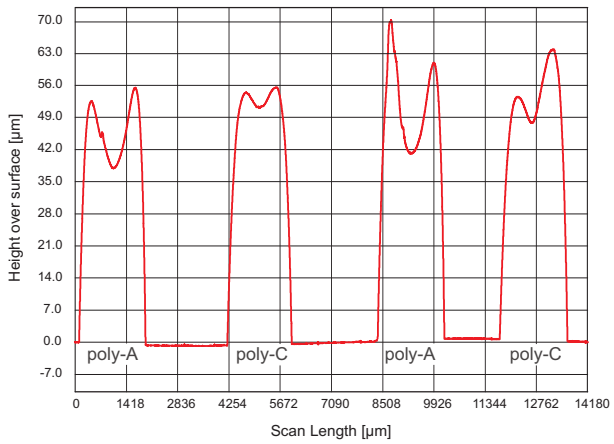

Fig. 9. Surface height profile of the sample FR-5 along the path indicated by the dashed line in Fig. 8.

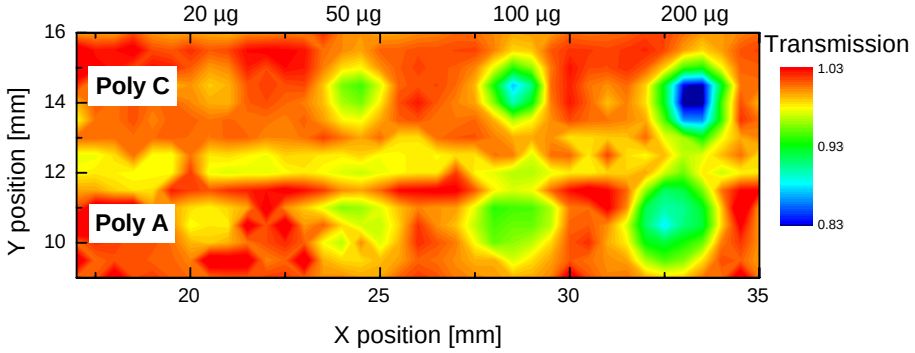

Fig. 10. THz transmission image of sample FR-6 prepared with poly-A and poly-C spots of varying mass, ranging from 20 μg to 200 μg.

A and poly-C. There is a clear difference in both absorption and index of refraction of the two polymers in the frequency range 0.1–3 THz, but we observe no characteristic resonances in the spectra. The sample material was prepared and characterized in two independent experimental setups, and the results obtained are in good agreement. We are therefore confident that the measured dielectric properties are directly related to the sample material.

We notice that our observation of resonance-free spectra of the RNA polymers are contradictory to observations made by Globus *et al.* [5]. In that work the authors observed many resonances in dried films of artificial RNA polymers, measured with a Fourier-transform infrared (FTIR) spectrometer. We believe that THz-TDS is a useful tool to ensure that observed features are related to the sample material since we directly measure both transmission amplitude and -phase. Therefore we can extract the absorption coefficient without resorting to estimates of the index of refraction. Equally important, the pulsed and time-resolved technique of THz-TDS allows us to identify and separate standing waves from the fundamental signal in the spectrometer. In other THz-region spectroscopic studies of large biomolecules [9, 10] is was also concluded that although distinct resonances are predicted by theory in the THz region, no spec-

#7174 - $15.00 USD
Received 15 April, 2005; revised 14 June, 2005; accepted 23 June, 2005

trally resolvable resonances were observed. The large spectral density of IR-active vibrational modes and the high sensitivity of the position of these modes to the local environment of the molecule leads to a continuous absorption profile basically following the spectral density of vibrational modes. Furthermore, compared to the narrow linewidth of vibrational modes expected for a molecule in vacuum low-frequency vibrational modes of molecules in the amorphous condensed phase will be strongly damped because of additional frictional terms originating from the presence of nearby neighboring molecules and the resulting weak intermolecular bonds.

For biological applications of THz spectroscopy the lack of distinct spectral resonances is a fundamental problem. For most, if not all, samples of biologically relevant macromolecules we expect that the *shape* of the THz absorption spectrum will be similar to the spectra presented here. However, by careful determination of the absolute absorption coefficient we still expect the THz region to offer important information about biologically relevant molecules and their aqueous environments. For example, the salinity and conductivity of electrolyte solutions was analyzed with THz spectroscopy by Asaki *et al.* [19] and THz absorption spectra showing a dependence on the conformation of the biomolecule was reported by Whitmire *et al.* [10].

We have shown that THz spectroscopy based on free-space propagation of the THz signal can be used to detect the presence of small amounts of dry sample material on a substrate, with a spatial resolution close to the diffraction limit given by the long wavelength of the THz radiation. The diffraction limit allows us to perform spectroscopy on spots of biomaterial larger than approximately 1 mm. In order to overcome the diffraction limit, and hence be able to perform spectroscopy on much smaller amounts of sample material, the confinement of the THz electric field is the key factor to address. Therefore the development of integrated THz technologies combined with sample delivery and handling systems is required. We envision rapid development in this direction within the next years, leading to strong advance of the field of biosensing with THz-frequency radiation.

Acknowledgments

This study was partially supported by the BMBF Biophotonics Program (FKZ 13N8313 and 13N8375) and the EU Program TeraNova (IST 2004-511415).

#7174 - $15.00 USD Received 15 April, 2005; revised 14 June, 2005; accepted 23 June, 2005